# A Novel Current Ripple Cancellation PWM

# for Isolated Three-phase Matrix DAB AC-DC Matrix Converter

Shunsuke Takuma, Keisuke Kusaka, Jun-ichi Itoh , *Yoshiya Ohnuma, *Satoshi Miyawaki
Nagaoka University of Technology/ *Nagaoka Power Electronics co., Ltd.
1603-1 Kamitomioka-chi Nagaoka city Niigata, Japan
Tel.,Fax: +81 / (258) – 47.9533.
E-Mail: takuma_s@stn.nagaokaut.ac.jp, itoh@vos.nagaokaut.ac.jp
URL http://itohserver01.nagaokaut.ac.jp/itohlab/index.html

## Keywords

«Matrix converter», «Three-phase system», «Modulation strategy», «Power factor correction», «Battery charger»

## Abstract

The control method for an isolated three-phase matrix dual active bridge (DAB) AC to DC converter is proposed to control sinusoidal grid current waveforms with a minimum reactive current. The conventional SVM based on a constant current is not applied to the isolated three-phase matrix DAB AC to DC converter due to a high di/dt by employing a leakage inductance. Therefore, the duty calculation for the matrix converter is required to approximate the waveforms at a high-frequency transformer or implement a numerical calculation. However, the gird currents are distorted due to the error by such approximation. In addition, the numerical calculation is used as a complex implementation and requires a long calculation time. In this paper, the novel modulation method based on the current ripple cancelation is proposed for the isolated three-phase matrix DAB AC to DC converter. The high di/dt ripple current against current reference is canceled by the sum of the currents during the positive and negative half switching cycle without the leakage inductance value. The input and output dc current controls are achieved considering the effects of the leakage inductance. A continuous current mode (CCM) and discontinuous current mode (DCM) on buck and boost modes are clarified and confirmed by simulation. As the simulation results, the input current THD is reduced by 88.2% compared with the conventional method. As experimental results, the input current THD of 3.8% is achieved at rated power with CCM and DCM operation.

## Introduction

In recent years, a demand for a rapid charger from a three-phase grid to a battery with galvanic isolation is increased. Requirements of a rapid charger are a constant output DC voltage, three-phase power factor correction (PFC) operation, and galvanic isolation between three-phase grid and battery side. In addition, downsizing and a weight reduction are also required. Generally, the isolated three-phase AC to DC converter employs a medium or high-frequency AC transformer to reduce the volume of the transformer. However, grid-tied inductors and smoothing capacitors maintaining a constant DC voltage prevent the downsizing of the system. Therefore, the isolated AC-DC converter using the matrix converter at the primary side has been studied [1]-[4]. A high-frequency voltage from a grid voltage is directly generated by the matrix converter. The downsizing and high efficiency are expected due to the elimination of the passive components such as e.g. the boost inductors and the DC-link capacitors.

In order to minimize further the system, the leakage inductance of the transformer is utilized such a DAB converter [5]-[6]. The control method for the isolated single-phase matrix DAB AC to DC converter is proposed in [7]-[8] based on the DAB control theory. However, the single-phase system is not suitable for the large capability application due to a high conduction loss compared with the three-phase system. In such isolated three-phase matrix DAB AC to DC converter, the control of the three-

phase to single-phase matrix converter at the primary side and the full bridge converter at the secondary side is required. Generally, the control of the isolated three-phase matrix DAB AC to DC converter is developed from the control theory for the dual active bridge (DAB) converter, which is based on the assumption that the input and output voltages are constant during one switching cycle. However, the input voltage of the isolated three-phase matrix DAB AC to DC converter changes according to the input voltage, which is the grid voltage. In addition, the high-frequency current has a high di/dt due to a leakage inductance of the transformer, leading to a nonlinear relationship between the duty and the transmission power. Therefore, the complex control algorithm is required to control the transmission power and the sinusoidal waveform at the input side. In order to simplify the duty calculation, the approximation of the output voltage of the matrix converter by the square waveform is proposed [9]. However, the input current distorts due to the error between the approximation waveform and the actual waveform. Meanwhile, the duty calculation with numerical analysis is proposed [10], which still results in a complex calculation. In [11]-[12], a simple control algorithm, which is the phase-shift control between the primary voltage and the secondary voltage has been proposed. However, the circulating current in the matrix converter increases compared with the control method of [10], resulting in the conduction loss increase.

In this paper, the control method for the isolated three-phase matrix DAB AC to DC converter is proposed to achieve the low input current distortion without a numerical calculation. The original idea of the proposed control method is that the AC current reference and periodic average current at the transformer are matched by the ripple cancellation of the active current during one switching period. The cancelation method is achieved by the selection of suitable output vector which is employed by the conventional SVM. In addition, the output vector is selected with the consideration of the minimization of the reactive current. It is confirmed that the low input current distortion is achieved by the proposed control method.

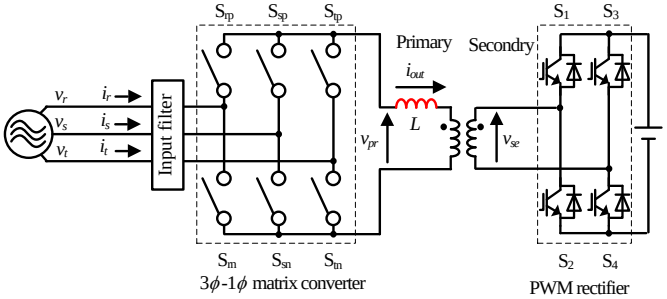


Fig. 1. High-frequency link matrix converter. This converter has a high di/dt because only small leakage inductor uses at the high-frequency transformer.

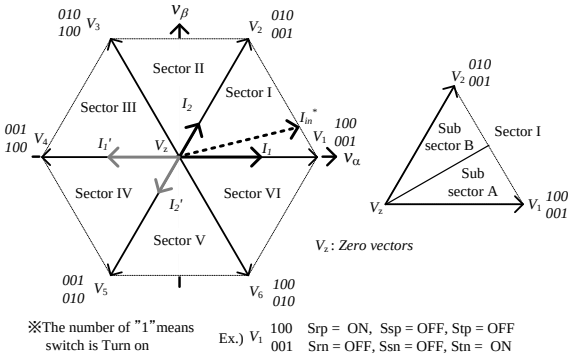


(a) Fundamental voltage vector diagram

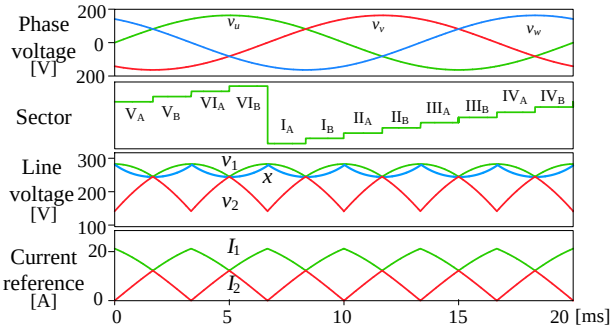


(b) Relationship between grid voltage and sector

Fig. 2. Fundamental space vector modulation.

## Principle of current ripple cancellation

Figure 1 shows the configuration of the isolated three-phase matrix DAB AC to DC converter. The full bridge converter at the primary side of a DAB converter is replaced by the matrix converter. In the control method for this topology, the leakage inductance of the high-frequency transformer is utilized. Consequently, the downsizing and the high efficiency of the system are achieved by removing both the smoothing inductor at the secondary side and the snubber circuit.

Figure 2(a) shows the fundamental voltage vector diagram and the reference current vector $I_{in}^*$. If the reference current vector $I_{in}^*$ is generated by $I_1$ and $I_2$, the input

current becomes sinusoidal when output voltage vectors $V_1$ and $V_2$ are selected.

$$I_1 = \frac{v_{2\beta} i_\alpha - v_{2\alpha} i_\beta}{v_{1\alpha} v_{2\beta} - v_{1\beta} v_{2\alpha}} \tag{1}$$

$$I_2 = \frac{v_{1\alpha} i_\beta - v_{1\beta} i_\alpha}{v_{1\alpha} v_{2\beta} - v_{1\beta} v_{2\alpha}} \tag{2}$$

where $v_{1\alpha}$, $v_{2\alpha}$, $i_\alpha$ and $v_{1\beta}$, $v_{2\beta}$, $i_\beta$ are alpha and beta components of $V_1$, $V_2$, and $I_{in}^*$. In this paper, the control method based on sector IA is explained. The other sectors operation are similar because the grid voltage relationships is symmetric in every 30 degree.

Figure 2(b) shows the relationship between the grid voltages and the selected sectors and vectors. Note that sectors and sub sectors are defined as Fig. 2(b) based on the grid voltages. The high-frequency output voltage vector is generated according to the sectors and the sub sectors.

**Conventional SVM**

Figure 3(a) shows the high-frequency waveforms at the transformer with the conventional SVM. It is assumed that two amplitudes at point A and B are equal to those at point A' and B', respectively. The output voltage vectors $V_1$ and $V_2$ are selected to output the positive voltage during the first half cycle. On the other hand, the output voltage vectors $V_4$ and $V_5$ are selected to output the negative voltage during the last half cycle. The solid line and dot line depict the instantaneous currents from point A to B and A' to B' during the transition of the output vectors $V_1$, $V_2$ and $V_4$, $V_5$ respectively. The instantaneous currents from point A to B and A' to B' during the positive and negative half cycle are same. As a result, the errors between the current reference and each actual average current occur during the duration $T_1$ and $T_2$

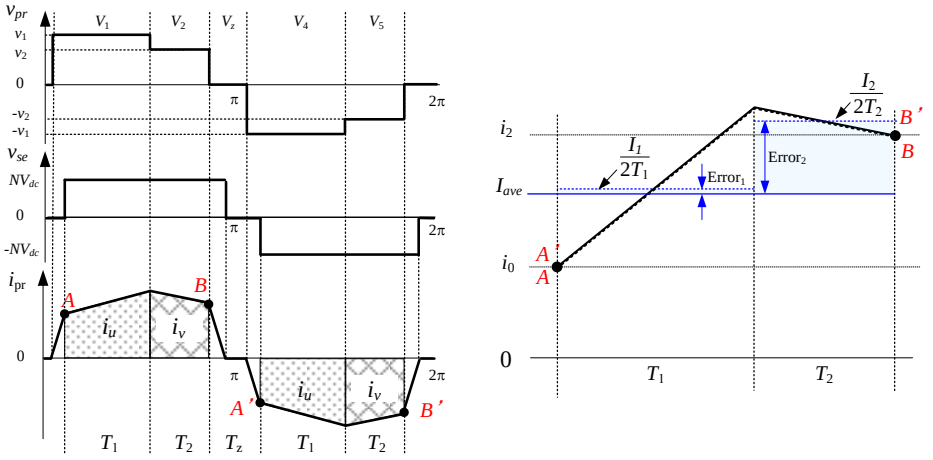


(a) Convectional method

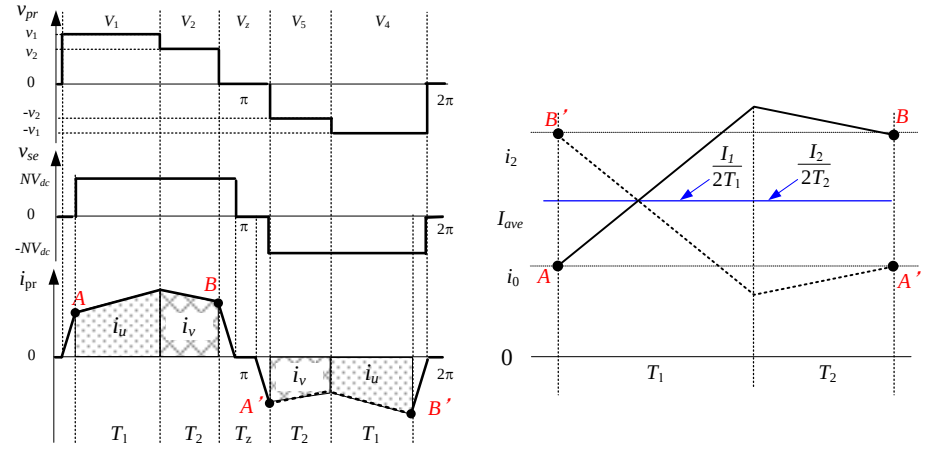


(b) Proposed current ripple cancellation method

Fig. 3. Effect of current ripple. The error between current reference and actual current occurs due to the current ripple with the conventional method. The current ripple during the positive cycle is canceled by them during the negative cycle with the proposed method.

because the ripple current is not ignored due to leakage inductance. Therefore, the conventional SVM is not suitable for the isolated three-phase matrix DAB AC to DC converter because the conventional SVM is based on constant output current during switching periods. In order to solve this problem, a complex algorithm or an offline calculation is required to include the effect of the current ripple. In this paper, the current ripple cancellation method is proposed to keep constant output current regardless of the small leakage inductance.

**Proposed SVM for current ripple cancellation**

Figure 3(b) depicts the ripple cancellation principle for the active current during one switching period. The instantaneous currents from point A to B and A' to B' during the positive and negative half cycle are different because the primary voltage during the negative cycle is changed to cancel the current ripple. The average currents $I_{ave1}$, $I_{ave2}$ during durations $T_1$, $T_2$ are expressed as

$$I_{ave1} = \frac{1}{2}\left\{ i_0 + \frac{v_{pr1} - NV_{dc}}{L} T_1 + i_2 - \frac{v_{pr1} - NV_{dc}}{L} T_1 \right\} \tag{3}$$

$$I_{ave2} = \frac{1}{2}\left\{ i_0 + \frac{v_{pr2} - NV_{dc}}{L} T_2 + i_2 - \frac{v_{pr2} - NV_{dc}}{L} T_2 \right\} \tag{4}$$

$$I_{ave} = I_{ave1} = I_{ave2} = \frac{i_0 + i_2}{2} \tag{5}$$

where, $v_1$ and $v_2$ are the output voltages during $V_1$ and $V_2$ respectively, $i_0$ is the initial current at $V_1$, and $i_2$ is the final state at $V_2$. The average current is independent of the high di/dt due to the leakage inductance. Therefore, the linearization between the input current reference and the duty are achieved to cancel the active current ripple during one switching periods. The primary and secondary voltages are generated by the matrix converter and the inverter based on the principle of the cancellation method.

## Control Strategy

In this section, the details of the proposed control method based on SVM and the switching pattern are explained.

Figure 4 shows the switching pattern for the matrix converter, the PWM rectifier and the operation waveforms at the transformer.

- $t_0$-$t_1$ The zero voltage at the primary side is generated by the short circuit operation between the upper and lower switches in one leg of the matrix converter, i.e.. $S_2$ and $S_3$ at the PWM rectifier turn on to clamp zero voltage
- $t_1$-$t_2$ The matrix converter outputs the maximum line to line voltage $v_1$ at the grid voltages. The secondary voltage is the negative voltage to minimize the reactive current. Next switching starts when the output current reaches to point A.
- $t_2$-$t_3$ The PWM rectifier outputs the positive voltage. This duty is decided by the current reference based on SVM.
- $t_3$-$t_4$ $S_{rp}$ and $S_{sp}$ of the matrix converter turns off and turns on. The power is transmitted from the grid side to DC side during $t_2$ to $t_4$.
- $t_4$-$t_6$ The maximum line to line voltage is selected to minimize the reactive current. Therefore, $S_{sp}$ and $S_{tn}$ of the matrix converter turn off. $S_{tp}$ and $S_{rn}$ of the matrix converter turn on.
- $t_6$-$t_7$ Both voltage at the primary and secondary side is maintained to zero to clamp zero current.

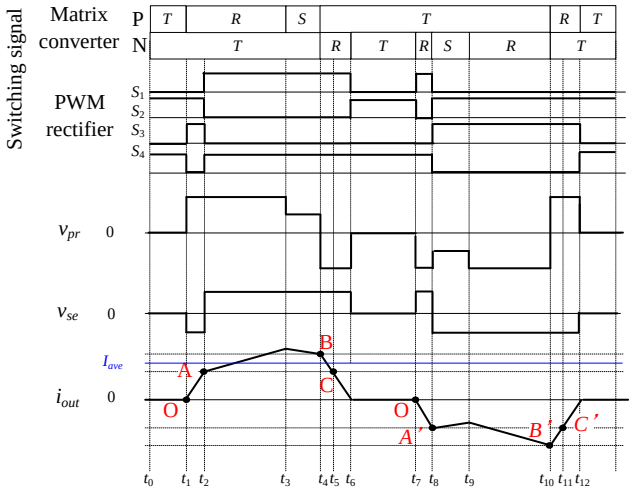


Fig. 4. Ripple cancellation principle for active current.

- $t_7$-$t_8$ The matrix converter outputs the maximum line to line voltage $v_1$ at the grid voltages. The secondary voltage is the negative voltage to minimize the reactive current. Next switching starts when the output current reaches to point A' which has the same amplitude of point A.
- $t_8$-$t_9$ the matrix converter outputs the medium line to line voltage $v_2$ to cancel the current ripple.
- $t_9$-$t_{10}$ $S_{sn}$ and $S_{rn}$ of the matrix converter turns off and turns on. ZVS when $S_{rn}$ turns on does not achieve because the drain-source voltage of $S_{rn}$ cannot be discharged due to the negative direction. However, the drain-source voltage of $S_{rn}$ is small voltage which is the differential voltage between the maximum and medium line to line voltage.
- $t_{10}$-$t_{12}$ In order to minimize the reactive current, the maximum line to line voltage is output from the matrix converter. Therefore, $S_{tp}$ and $S_{rn}$ of the matrix converter turn off. $S_{rp}$ and $S_{tn}$ of the matrix converter turn on.

Figure 5(a) and (b) show a high frequency current waveform with the current ripple cancellation. The operation modes are separated into two modes such as buck mode and boost mode depending on the grid voltages and DC voltage. The sign function is defined as

$$sign(x)=\begin{cases}1 & x>NV_{dc}\\ -1 & x<NV_{dc}\end{cases} \qquad x=\frac{v_1I_1+v_2I_2}{I_1+I_2} \tag{6}.$$

The average current $I_{ave}$ during point A to B is defined as the equivalent transformer current reference $I_{ave}^*$ in the powering mode. Each duty of $I_1$ and $I_2$ expressed as

$$D_1=\frac{I_1}{I_{ave}^*}-sign(x)D_z \tag{7},$$

$$D_2=\frac{I_2}{I_{ave}^*} \tag{8}.$$

where $D_z$ is the compensation duty for $D_1$. The current during $T_z$ is a reactive or active current in the buck or boost mode. Therefore, addition or subtraction from $D_1$ is required to compensate the effect of the current during $T_z$. As shown in Figure 4(b), the sum of the output current, which is from point 0 to A and from point 0 to B, is double of $I_{ave}^*$ and is expressed as

$$2\frac{(v_1+NV_{dc})}{L}T(D_\alpha-\frac{1}{2}D_z(1+sign(x)))+\frac{(v_1-NV_{dc})}{L}TD_1+\frac{(v_2-NV_{dc})}{L}TD_2=2I_{ave}^* \tag{9}$$

where $L$ is the leakage inductance referred to the primary side of the transformer, $V_{dc}$ is the DC voltage. Solving the equation (8), $D_a$ is expressed as

$$D_\alpha=\frac{2I_{ave}^*\frac{L}{T}-(v_1-NV_{dc})D_1-(v_2-NV_{dc})D_2}{2(v_1+NV_{dc})}-\frac{1}{2}D_z(1+sign(x)) \tag{10}.$$

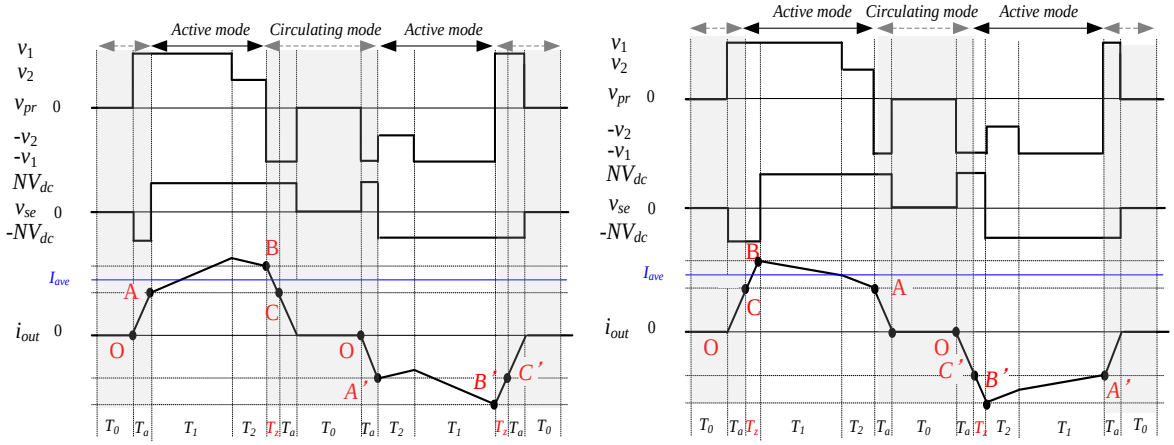


(a) Buck mode $v_1>NV_{dc}>v_2$ (b) Boost mode $NV_{dc}>v_1>v_2$

Fig. 5. Ripple cancellation principle for active current.

$D_z$ is decided to equalize the amount of the change during $T_1$ to $T_2$ respectively.

$$D_z = sign(x)\frac{(v_1 - NV_{dc})I_1 + (v_2 - NV_{dc})I_2}{2NV_{dc}I_{ave}^*} \tag{11}$$

Substring (11) into (6), $D_1$ is expressed by

$$D_1 = \left\{\frac{I_1}{I_{ave}^*}\frac{(V_2 - V_{out})D_2}{V_1 + V_{out}}\right\}\frac{(V_1 + V_{out})}{2V_{out}} \tag{12}$$

Finally, the zero current period $D_0$ is defined by

$$D_0 = 1 - (2D_\alpha + D_1 + D_2 + D_z) \tag{13}$$

The equivalent transformer current reference $I_{ave}^*$ is restricted by the switching frequency, the leakage inductance $L$, the grid voltage, and the DC voltage. The equivalent transformer current reference is expressed as

$$I_{ave}^* = \frac{1}{2}\left\{(1 - D_0)\frac{v_1 + NV_{dc}}{2}\frac{T}{L} - \sqrt{\left(\frac{v_1 + NV_{dc}}{2}\frac{T}{L}\right)^2 - \frac{v_1 + NV_{dc}}{2}\frac{I_1(v_1 + NV_{dc}) + I_2(v_2 + NV_{dc})}{NV_{dc}}\frac{T}{L}}\right\} \tag{14}$$

In CCM, the zero current period is keep to zero. Therefore, the current reference for CCM is expressed as

$$I_{ave}^* = \frac{1}{2}\left\{\frac{v_1 + NV_{dc}}{2}\frac{T}{L} - \sqrt{\left(\frac{v_1 + NV_{dc}}{2}\frac{T}{L}\right)^2 - \frac{v_1 + NV_{dc}}{2}\frac{I_1(v_1 + NV_{dc}) + I_2(v_2 + NV_{dc})}{NV_{dc}}\frac{T}{L}}\right\} \tag{15}$$

On the other hands, the high frequency current has zero current periods in the DCM which is operated under $D_a$=0. Therefore, the zero current period $D_0$ is expressed as

$$D_0 = 1 - \frac{I_1 + I_2}{I_{ave}^*} \tag{16}$$

The current reference for the DCM is expressed as

$$I_{ave}^* = \sqrt{sign(x)\frac{v_1 + NV_{dc}}{4NV_{dc}}((v_1 - NV_{dc})I_1 + (v_2 - NV_{dc})I_2)\frac{T}{L}} \tag{17}$$

The current references for CCM and DCM are same at the boundary condition. Substituting (17) into (15), the transition power at the boundary condition is expressed as

$$P_{b\_buck} = \frac{\pi NV_{dc}}{4\sqrt{6}v_{ac}}\frac{3{v_{ac}}^2 - 2N^2{V_{dc}}^2}{\omega L} \tag{18},$$

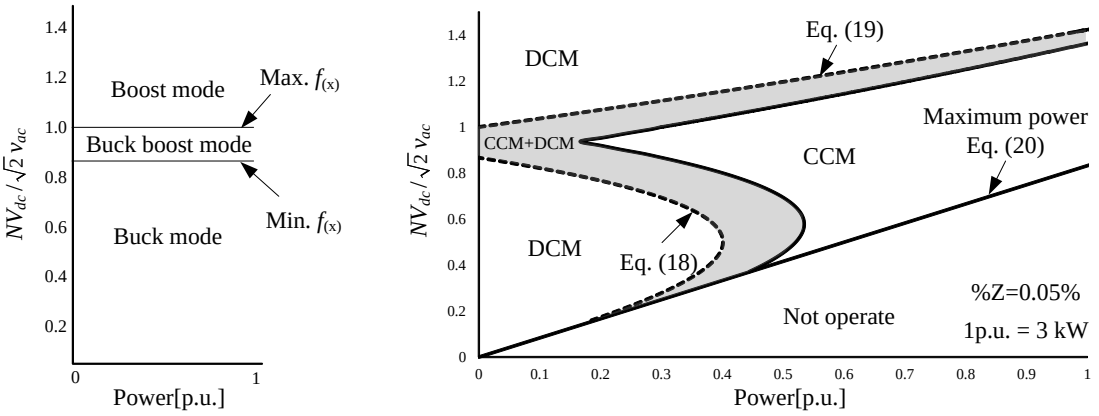


(a) Operation modes (b) Boundary conditions

Fig. 6. Relationship between maximum transition power and input and output voltage. The operation mode and current mode are changed by the grid voltage, DC voltage and transition power.

$$P_{b\_boost} = \frac{\pi v_{ac}}{2\sqrt{2}NV_{dc}} \frac{N^2 V_{dc}^{\ 2} - 2v_{ac}^{\ 2}}{\omega L} \quad (19)$$

where $v_{ac}$ is the RMS value of the grid voltage. The equations (18) and (19) express the boundary condition without CCM during 0 to 30 degree completely. Solving (14), the maximum transition power $P$ is expressed as

$$P = \frac{\pi\sqrt{6}}{16} \frac{v_{ac} NV_{dc}}{\omega L} \quad (20)$$

Changing (20), the leakage inductance is calculated by using (21).

$$L \le \frac{\pi\sqrt{6}}{16} \frac{v_{ac} NV_{dc}}{\omega P} \quad (21)$$

Figure 6(a) shows the operation mode of the isolated three-phase matrix DAB AC to DC converter. It is assumed that the turn ratio of the transformer is 1. The matrix converter is operated under the boost mode when the DC voltage is larger than the maximum line to line voltage. On the other hands, the matrix converter is operated under the buck mode when the DC voltage is lower than 0.866 times of the maximum line to line voltage.

Figure 6(b) shows the boundary conditions between CCM, DCM and mixed CCM and DCM during the grid period. %Z of the leakage inductance is designed to 0.05%. According to (20), the transition power is restricted by the switching frequency, the leakage inductance, the grid voltage, the DC voltage, and the turn ratio. A DAB converter for the DC-DC conversion has the similar limitation by the same circuit parameter. The high-frequency current has zero current period in DCM when the DC voltage is significantly larger or lower than the grid voltage at a light load.

## Simulation and Experimental Results

Table 1 shows the simulation and experimental conditions. The four-step voltage commutation is applied to avoid the short-circuit for the matrix converter. Each dead-time for the matrix converter and the PWM rectifier is set to 250 ns depending on the rise and fall time of the switching device (ROHM SCT2080KE).

Figure 7 shows the input voltages and currents of the matrix converter and the waveforms at the transformer without the commutation and the input filter to confirm the validity of the proposed control method at light

Table I Simulation and experimental conditions

| Element | Symbol | Value |
|---|---|---|
| Rated power | $P$ | 3.0 kW |
| Three-phase AC voltage | $v_{ac}$ | 200 V |
| DC voltage | $V_{dc}$ | 120 V |
| Input frequency | $f$ | 50 Hz |
| Carrier frequency | $f_{sw}$ | 20 kHz |
| Leakage inductance | $L(\%Z)$ | 45 μH(0.2%) |
| Turn ratio of transformer | $N_1$:$N_2$ | 2:1 |
| Input filter | $L_f$ | 1 mH |
| | $C_f$ | 10 μF |
| Dead-time | $T_d$ | 250 ns |

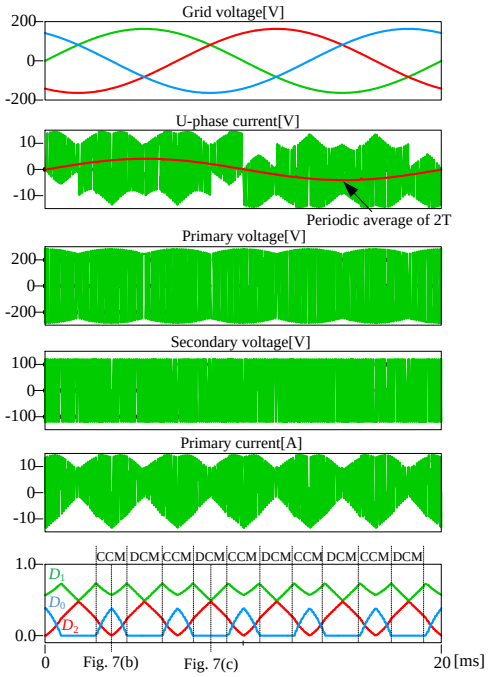


(a) operation waveforms

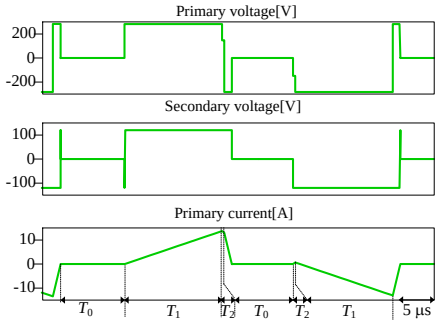


(b) DCM

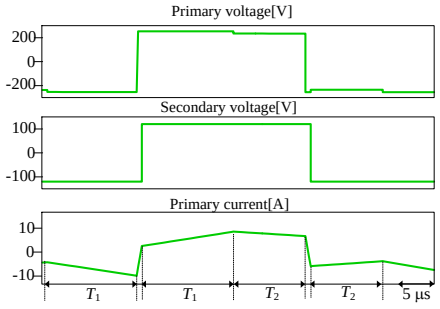


(c) CCM

Fig. 7. High-frequency voltage and current waveforms at transformer.

load (0.2 p.u.). The operation mode is changed by (6) from CCM to DCM during 6 times of the grid frequency. It is confirmed that the input current is not distorted by changing two mode because each duty can be calculated at the peak or bottom of the carrier. The input current is controlled to the sinusoidal waveforms and unity power factor. Fig. 7(b) and (c) shows the high frequency waveforms at the transformer with CCM and DCM. The each operation mode is changed by the relationship between the instantiations line to line voltage and DC voltage. In DCM, the primary and secondary voltage is controlled to keep the zero voltage when the current at the transformer is zero. On the other hand, the current at the transformer is operated in CCM.

Figure 8(a) and 8(b) show the simulation results of the actual and reference phase-current with the conventional method [10] and the proposed method, respectively. The input current filter uses the periodic average filter by the switching frequency without the LC filter to confirm each theory. In Fig. 8(a), the actual input current follows the command only when the approximated square waveforms and actual waveforms are matched. However, the input current distorts due to the error which is not ignored when the approximated square waveforms and actual waveforms are different. In Fig. 8(b), the actual current completely follows the command with the proposed current ripple cancelation method. It is confirmed that the grid current is controlled to keep the sinusoidal waveforms by the proposed method.

Figure 9 shows the comparison results of THD characteristics between the conventional and proposed method with the LC filter. The input current THD characteristics of the conventional method and the proposed method. The input current THD with the conventional method is over than 15.0% under the any load condition due to the approximation error. The THD requirement for the grid connection is not satisfied at rated power. It is difficult to improve THD by a compensation such as feed-forward because the error between the actual current and current reference is nonlinear. On the other hand, the input current distortion with the proposed method is greatly reduced by 88.2% from 17.0% to 2.0% compared with the conventional method [10]. In addition, the duty for each converter is decided by the equation without a numerical calculation and off-line calculation. The input current THD which is lower than 5% is achieved over the load range from 0.3p.u. to 1.0p.u.

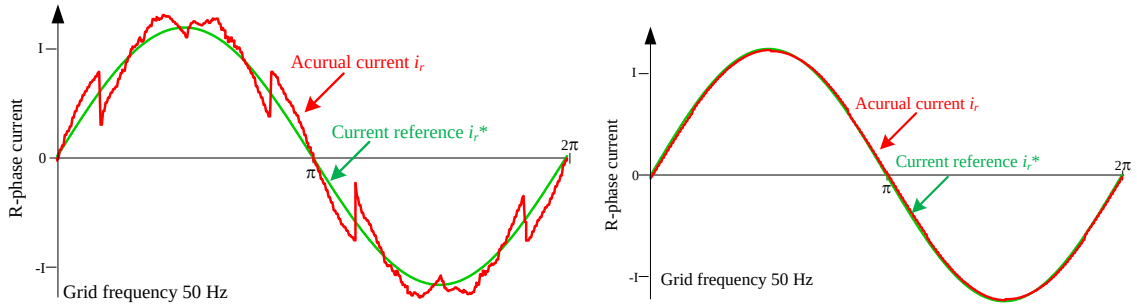


Conventional control method Proposed control method

Fig. 8. Simulation results of actual value and command. The input filter is the periodic filter of the switching frequency. The input current reference and the actual current are completely matched with the application of the proposed method.

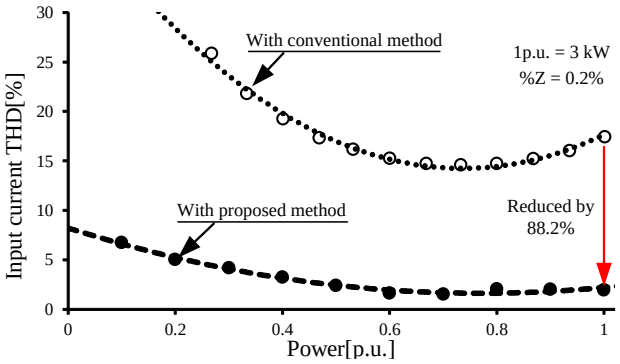


Fig. 9. THD characteristics without commutation. The input current THD is suppressed by 88.2% to apply the proposed method. The input current is controlled to keep the low distortion which is lower than 5% over the input power from 0.3p.u. to 1.0p.u..

Figure 10(a) shows the experimental results of the input and output waveforms of the matrix converter at rated power. The input current THD of 3.8% and the unity power factor are achieved by the application of the proposed method, satisfying the grid harmonic constraints. Figure 11(b) shows the extended waveforms of Fig. 11(a). It is confirmed that the output voltage waveforms are similar between the experimental and simulation results.

Figure 11(a) and (b) show the primary side voltage, secondary side voltage and primary side current at the transformer in DCM and CCM at the light load. In DCM, the primary current is maintained to zero current when the primary voltage and secondary voltage is zero voltage in theory. However, the primary current has the offset of 2A due to the effect of the dead-time. The actual switching timing is delayed by the dead-time depending on the direction of the high-frequency output current. The dead-time compensation will be implemented to improve the input current THD. In Fig. 11(b), the output current is controlled to remove zero current period to minimize the reactive current. Therefore, the zero voltage period is also removed from the primary voltage and secondary voltage for CCM

## Conclusion

The control method for the isolated three-phase matrix DAB AC to DC converter, which consisted of the matrix converter and the PWM rectifier was proposed. The current ripple during one switching period was cancelled by the sum of the ripple current during the positive and negative half switching cycle without the leakage inductance value. Therefore, the current ripple cancellation method was not required to calculate the complex duty because the duty was calculated by SVM based on constant output current. The active current was controlled with the ripple cancellation due to the leakage inductance of the transformer. The boundary conditions between CCM and DCM on the buck and boost mode were employing by the improvement of the efficiency with a pulse frequency modulation at light load. By applying the proposed method, the input current THD at rated load was suppressed by 88.2%

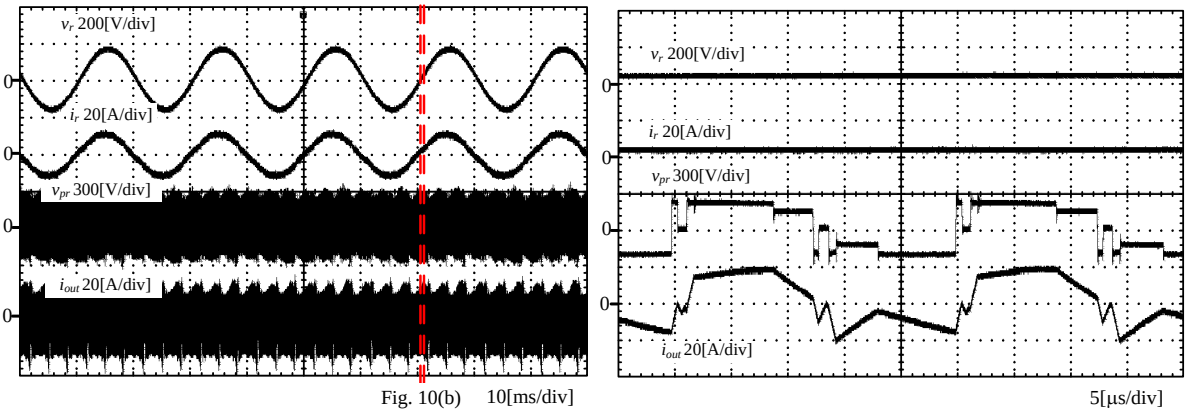


(a) Operation waveforms (b) Extended waveforms of Fig. 10(a)

Fig. 10. Experimental results of input and output waveforms. The input current THD of 3.8% is achieved by the proposed method.

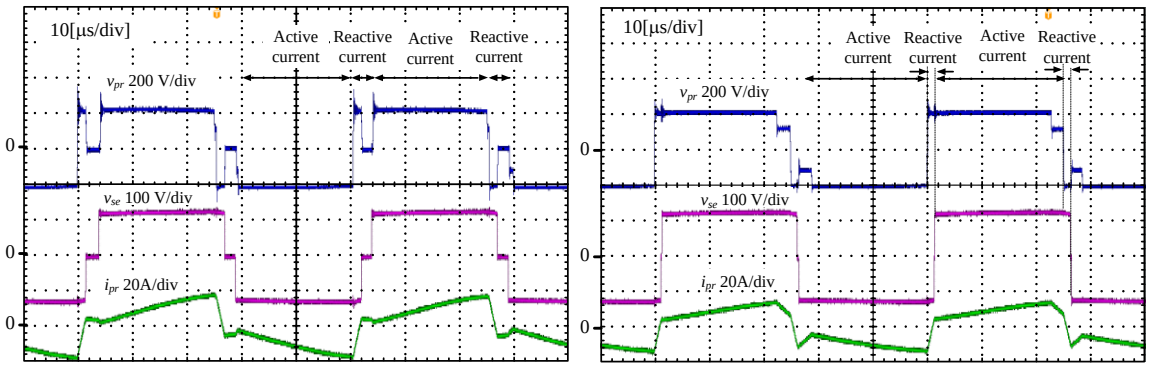


(a) Discontinues current mode (b) Continues current mode

Fig. 11. Operation waveforms at high frequency transformer. (P=0.2 p.u.)

in the simulation. As experimental results, the input current THD is 3.8% at rated power in CCM and DCM.

## References


[1] V. Vlatkovic, D. Borojevic, X. Zhuang and F. C. Lee, "Analysis and design of a zero-voltage switched, three-phase PWM rectifier with power factor correction," PESC '92 Record. 23rd Annual IEEE Power Electronics Specialists Conference, Toledo, Spain, 1992, pp. 1352-1360 vol.2.

[2] V. Vlatkovic, D. Borojevic and F. C. Lee, "A zero-voltage switched, three-phase isolated PWM buck rectifier," in IEEE Transactions on Power Electronics, vol. 10, no. 2, pp. 148-157, March 1995.

[3] Z. Yan, M. Jia, C. Zhang and W. Wu, "An Integration SPWM Strategy for High-Frequency Link Matrix Converter With Adaptive Commutation in One Step Based on De-Re-Coupling Idea," in IEEE Transactions on Industrial Electronics, vol. 59, no. 1, pp. 116-128, Jan. 2012.

[4] C. Li, Y. Zhong and D. Xu, "Soft-switching three-phase matrix based isolated AC-DC converter for DC distribution system," 2015 IEEE Energy Conversion Congress and Exposition (ECCE), Montreal, QC, 2015, pp. 6755-6761.

[5] Muhammad Hazarul Azmeer bin Ab Malek, Hiroaki Kakigano, and Kiyotsugu Takaba, "Dual Active Bridge DC-DC Converter with Tunable Dual Pulse-Width Modulation for Complete Zero Voltage Switching Operation,"IEEJ Journal of Industry Applications, vol. 8, no. 1, pp. 98-107, 2019.

[6] Muhammad Hazarul Azmeer bin Ab Malek, Hiroaki Kakigano, and Kiyotsugu Takaba"Combined Pulse-Width Modulation of Dual Active Bridge DC-DC Converter to Increase the Efficiency of Bidirectional Power Transfer,"IEEJ Journal of Industry Applications, vol. 7, no. 2, pp. 166-174, 2018.

[7] N. D. Weise, G. Castelino, K. Basu and N. Mohan, "A Single-Stage Dual-Active-Bridge-Based Soft Switched AC–DC Converter With Open-Loop Power Factor Correction and Other Advanced Features," in IEEE Transactions on Power Electronics, vol. 29, no. 8, pp. 4007-4016, Aug. 2014.

[8] F. Jauch and J. Biela, "Combined Phase-Shift and Frequency Modulation of a Dual-Active-Bridge AC–DC Converter With PFC," in IEEE Transactions on Power Electronics, vol. 31, no. 12, pp. 8387-8397, Dec. 2016.

[9] M. A. Sayed, K. Suzuki, T. Takeshita and W. Kitagawa, "Soft-Switching PWM Technique for Grid-Tie Isolated Bidirectional DC–AC Converter With SiC Device," in IEEE Transactions on Industry Applications, vol. 53, no. 6, pp. 5602-5614, Nov.-Dec. 2017.

[10] K. Shigeuchi, K. Sakuma, J. Xu, N. Shimosato and Y. Sato, "A New Modulation Method for a Bidirectional Isolated Three-Phase AC/DC Dual-Active-Bridge Converter to Realize Higher Efficiency in Wide Output Voltage Range," 2018 IEEE Energy Conversion Congress and Exposition (ECCE), Portland, OR, 2018, pp. 592-598.

[11] D. Varajão, R. E. Araújo, L. M. Miranda and J. A. P. Lopes, "Modulation Strategy for a Single-Stage Bidirectional and Isolated AC–DC Matrix Converter for Energy Storage Systems," in IEEE Transactions on Industrial Electronics, vol. 65, no. 4, pp. 3458-3468, April 2018.

[12] D. Das, N. Weise, K. Basu, R. Baranwal and N. Mohan, "A Bidirectional Soft-Switched DAB-Based Single-Stage Three-Phase AC–DC Converter for V2G Application," in IEEE Transactions on Transportation Electrification, vol. 5, no. 1, pp. 186-199, March 2019.

[13] A. K. Singh, P. Das and S. K. Panda, "Novel switching scheme for matrix based isolated three phase AC to DC conversion," IECON 2014 - 40th Annual Conference of the IEEE Industrial Electronics Society, Dallas, TX, 2014, pp. 3324-3329.